'89 KACC 1989. 10. 27~28

A Study On Peg and Hole Assembly Using RCC

Katsutoshi Kuribayashi, Shigenobu Kishi, Toshiro Ono

University of Osaka Prefecture,

804 Mozu-Umemachi 4-Cho, Sakai, Osaka 591 JAPAN

ABSTRACT

RCC(=Remote Center Compliance)[1][2] is a useful device for peg and hole insertion works. Two methods for smooth insertion of round peg and round hole are proposed. The idea of method 1 is to design the optimum position of the compliance center of RCC which is different from that of usual RCC in order to minimize the insertion force with the assumption of the known insertion angle. The idea of method 2 is to insert peg with rotation in order to decrease the friction coefficient between peg and hole. The two ideas are analyzed theoretically and are shown valid experimentally.

1. INTRODUCTION

RCC(=Remote Center Compliance)[1][2] is a useful device for aiding assembly insertion operations. Its major function is to act as a flexible shaft allowing positional and angular misalignment between parts to be assembled. However, generally even if this device is used for assembly, the insertion force doesn't become zero because of the friction between two parts. This force cause the assembly time consumption which increase the assembling cycle time, needs a bigger power manipulator and may happen to hurt to parts. Thus the insertion force should be decreased for more excellent RCC with smooth and short time insertion.

In this paper, a study on a round peg and round hole assembly using conventional RCC has been done to find conditions for decreasing the insertion force in the assembly. The methods are based on the following ideas: 1) The insertion force has minimum concerned with the position of the compliance center(=CC) which is fixed at the peg's tip center for the usual RCC. 2) Rotating peg around its axis decreases the insertion force. In the idea 1), it should be assumed that the insertion angle between peg and hole axes is known although this is not assumed for the usual RCC. On the other hand, the second idea 2) doesn't need this assumption. The proposed two methods are analyzed theoretically, and the design method for these ideas are derived. Moreover, the insertion experiments of peg and hole were carried. As the results, the theories are proved fit for the experiments and the two methods are shown valid.

NOMENCLATURE

c : clearance ratio between peg and hole
d : peg diameter
D : hole diameter
f : friction force
Fx : force along the X axis at the peg tip
Fz : force along the Z axis at the peg tip
Kx : lateral stiffness around compliance center
K_θ : angular stiffness around compliance center
ℓ : insertion depth
Lg : distance between compliance center and peg tip (positive for peg tip under compliance center)
M : moment at peg tip (positive counter clockwise)
r : = d/2
R : = D/2
U : horizontal distance from compliance center to center line of hole
W : chamfer width
z : chamfer crossing
α : chamfer angle
ε : horizontal error from peg's tip center to center line of hole (positive with peg's tip center left from center line of hole)
θ : angular error between peg and hole (positive counter clockwise)
μ : dynamical friction coefficient

2. PRINCIPLE of RCC

Fig.1 shows the 2 dimensional model of RCC. Usually the top of RCC is connected with an industrial manipulator, and a peg is grasped at the bottom of RCC. The parts B and C in RCC are composed of the flexible end points which are connected with another parts and the rigid main bodies. Therefore, applying a horizontal force at the peg's tip, the peg's tip center O moves horizontally, because B is deformed at its ends and the parts B are declined parallel. At that time, parts C can not be deformed since the cross point of the productions of parts B is at the peg's tip center.

On the other hand, applying moment around the peg's tip center, the peg rotates around the peg's tip center O because parts C are deformed at their end, but parts B can not be deformed. As mentioned above, the compliance center is defined as the point at which the horizontal movement and rotation are independent for the applied horizontal force and moment . In other expression, at the compliance center, the next equation holds.

$$\begin{bmatrix} F \\ M \end{bmatrix} = \begin{bmatrix} K_x & 0 \\ 0 & K_\theta \end{bmatrix} \begin{bmatrix} x \\ \theta \end{bmatrix} = \underline{K} \begin{bmatrix} x \\ \theta \end{bmatrix}$$

Namely, the rigidity matrix becomes diagonal.

For the case a peg is inserted into a hole, the above functions of RCC are very useful,that is, the horizontal error between the peg and hole will be decreased with the insertion depth because the force caused by its error drives the peg's tip center horizontally, and moreover the angular error will be decreased by the moment acting around the peg's tip center. Fig.2(b) shows their movement mechanism mentioned above.

Fig.2(a) and (c) shows the insertion mechanisms by the RCC with the $Lg>0$ and $Lg<0$, respectively.

Fig.2(a) shows the insertion mechanism that the angular error doesn't decrease but increases though the horizontal error decreases. On the other hand, if the insertion is done from the right hand chamfer of peg and hole, both the horizontal and angular errors decrease and after crossing chamfer the angular error is also corrected.

Fig.2(c) shows that both the horizontal and angular errors can decrease and moreover after the chamfer crossing the angular error can be corrected. On the contrary, if the peg is inserted at the right chamfer, the angular error will increase although the horizontal error decreases.

3. FUNDAMENTAL EQUATIONS of RCC

Referring to the reference [2], the basic equations for the insertion forces between peg and hole will be explained for three insertion processes. Several variables and parameters are shown in Fig.3. A hypothesis for deriving these equations is " θ is small ".

(1) Chamfer crossing

The insertion force Fz for chamfer crossing is obtained as follows.

$$F_z = \frac{Kx\ K_\theta A}{(K_x Lg^2 + K_\theta)\ B - K_x Lg\ r\ A} \times \frac{z}{\tan \alpha} \quad (1)$$

The insertable condition for chamfer crossing is expressed by next inequality.

$$| \varepsilon_\theta | < W_1 + W_2 \quad (2)$$

(2)One point contact

The insertion force Fz for one point contact can be derived.

$$F_z = \frac{\mu K_x K_\theta (\varepsilon_\theta' + \ell \theta_\theta)}{C (Lg - \ell) + K_\theta} \quad (3)$$

where

$$\varepsilon_\theta' = \varepsilon_\theta - cR \quad (4)$$

$$C = K_x (Lg - \ell - \mu r) \quad (5)$$

(3) 2 points contact

Fig.4 shows the two points contact between peg and hole. Based on Fig.4. The insertion force Fz for two points contact can be derived.

$$F_z = \frac{2\mu}{\ell}\left[E\left(\theta_\theta - \frac{cD}{\ell}\right) + F \right] + \mu\left(1 + \frac{\mu d}{\ell}\right)\left[G\left(\theta_\theta - \frac{cD}{\ell}\right) - \frac{F}{Lg} \right] \quad (6)$$

where

$$E = K_x Lg^2 + K_\theta\ ,\ F = K_x Lg\, \varepsilon_\theta''\ ,\ G = -K_x Lg \quad (7)$$

For preventing the jamming, the next conditions are necessary.

$$\frac{F_x}{F_z} \leqq \frac{1}{\mu} \quad (8)$$

$$\left| \frac{M}{rF_z} + \mu(1 + \lambda)\frac{F_x}{F_z} \right| < \lambda \quad (9)$$

Moreover, for preventing the wedging, the next inequality is necessary.

$$| \theta | < \frac{c}{\mu} \quad (10)$$

4.MINIMUM INSERTION FORCE DESIGN METHOD

Minimum insertion force design method to decrease the insertion force of peg and hole than the usual RCC will be proposed in this chapter. The position of CC to make the insertion force minimum will be analyzed theoretically based on the fundamental theory in the before chapter, assuming the insertion angle between peg and hole known.

Fig.5 shows the insertion force Fz vs. the insertion depth for the position of CC, Lg=15,-15 and -30, the insertion angle $\theta_o = 0.0167$rad, These insertion forces were calculated by eqs. (1),(3) and (6). From this figure, it is observed that the insertion force Fz for Lg=-15 is smaller than that of RCC, Lg=0, although the insertion force Fz for Lg=15 is larger than that of RCC. The above insertion situation is the same as that shown in Fig.2(c) whose insertion begins from the left chamfer. However, since the insertion force for Lg=-30 increase comparing to that for Lg=-15, it is understood that there is a minimum insertion force according to Lg.

The above fact will be analyzed theoretically below. Referring to Fig.5, in order to decrease the insertion force, the maximum insertion force respect to the insertion depth should be minimized according to Lg. Thus, the minimum insertion force Fz* can be expressed as follows.

$$Fz^* = \min_{Lg} \max_{\ell} Fz \tag{11}$$

Since $\max_{\ell} Fz$ happens during two points contact process, the maximizing insertion depth l^* can be gotten by maximizing Fz indicated by (6). Therefore l^* is the solution of the next equation.

$$\frac{dFz}{d\ell} = 0 \tag{12}$$

Then

$$\ell^* = \frac{(4E + 2G\mu d)cD}{2E\theta_0 + F(2 - \mu d/Lg) + G(\theta_0 \mu d - cD)} \tag{13}$$

Next Lg^* minimizing $\max_{\ell} Fz$ can be obtained by the next equation, differentiating (6) in which above l^* is inserted.

$$\frac{dFz(l^*(Lg),Lg)}{dLg} = 0 \tag{14}$$

For example, using (14) with known parameter shown in Fig.6, the optimum Lg^* was calculated as the function of θ_0 and is shown in Fig.6. From this figure, except for $\theta_0=0$, at which $Lg^*=0$, that corresponds to the condition of the usual RCC, optimum Lg^* is always smaller than zero. This means the insertion force is smaller than that of the usual RCC. The above insertion condition corresponds to that shown in Fig.2(c) whose insertion begins at the left chamfer.

5. SMALL INSERTION FORCE DESIGN METHOD

Small insertion force design to decrease the insertion force by decreasing the insertion friction coefficient between peg and hole will be proposed, using the usual RCC whose CC is at the peg's tip center, with unknown insertion angle.

Referring to (6) , the insertion force Fz is approximately the linear function of the friction coefficient μ . Thus it can be expected that the insertion force decreases linearly according to decreasing μ . Moreover,from (8)-(10) it can be expected that the smaller the friction coefficient, the wider the feasible insertion condition.

The idea of the insertion force method proposed here is to insert peg into hole with peg's rotation like a insertion of a screw. During insertion of peg into hole, insertion velocity Vz and rotary speed Vc along the circular arc of the surface of peg can be expressed as shown in Fig.7(a), where ψ is a screw angle. Another expression of ψ can be gotten as shown in Fig.7(b),where p is a screw pitch in a screw insertion. Thus, the next relationship between the velocities and the geometrical dimensions of a screw can be gotten.

$$\frac{Vc}{Vz} = \frac{\pi D}{p} \tag{15}$$

From Fig.7(b),

$$\sin\psi = \frac{p}{\sqrt{(\pi D)^2 + p^2}} \tag{16}$$

is obtained.

If normal force f_N on the surface of hole acts on its arbitrary contact point, the friction force between them due to f_N is μf_N in which μ is the usual dynamic friction coefficient defined before. The direction of μf_N is along $\bar{V}$ shown in Fig.7(a). This force μf_N can be decomposed to the components of the insertion and rotary arc directions as shown in Fig.7(c). From this consideration, the observed insertion force Fz can be obtained as follows.

$$Fz0 = \mu \sin\psi \cdot fN \tag{17}$$

This equation means that the insertion force with peg rotation becomes $\sin\psi$ times the usual insertion force by the usual RCC. It is known the faster the rotary speed Vc, the smaller the friction coefficient. However, because increasing the rotary speed results increasing the loss energy which will be converted into heat energy, due to $\bar{V} \times \mu f_N$, the problem of heat will limit the rotary speed .

Defining the observed friction coefficient μ' as

$$\mu' = \mu \sin\psi \tag{18}$$

,the insertion force Fz for this rotary insertion can be obtained by using μ'instead of μ in the before equations.

For example, the insertion forces calculated by using (6) for Vc/Vz = 2.5 is shown in Fig.8 with the insertion force by no rotary insertion. For this case, the observed friction force is 0.1 times the usual insertion force. From this result, it is expected that peg rotation is very effective to decrease the insertion force.

6. EXPERIMENTS

The experiments were carried out to prove the proposed methods valid.

The schematic diagram of the experimental system is shown in Fig.9. RCC is attached to the end of a manipulator with 6 degrees of freedoms to drive RCC vertically. A peg is fasten to the bottom surface of RCC by a screw. A hole is made in the steel block. The insertion forces were measured by the strain gage attached to the frame to support the steel block.

6.1 Experiment 1

Experiment 1 was carried out to prove the method proposed in 4 valid.

First, the theoretical insertion forces corresponding to the experiment were calculated by (1),(3) and (6), using parameters in Table 1, 2 and Fig.10,11, for 3 pegs, and are shown in Fig.12. This case corresponds to that shown in Fig.2 whose insertion begins from the left chamfer. Fig.12(a) shows the insertion force for Lg<0 is smaller than that for Lg>0.

The corresponding experiment was carried out and the results are shown in Fig.12(b).

Comparing the two results shown in Fig.12(a) and (b), the experimental insertion forces don't coincide very well with the theoretical ones. The reasons may be due to the setting error between peg and hole, the lack of precision of the manipulator and unpredicted friction coefficient. However, the order of the experimental insertion forces is the same as that of the theoretical ones, and moreover the shapes of the curves of the experimental insertion forces are very similar with those of the theoretical insertion forces. Therefore, it is proved that the idea of the minimum insertion force design method is correct, and its method is valid.

From the above results, the proposed method to decrease the insertion friction force is proved to be valid experimentally.

6.2 Experiment 2

To prove the small insertion force design method valid, the experiment 2 was carried out.

The experimental results is shown in Fig.13, under the experimental conditions which is the same as the conditions in Fig.8.

From Fig.13, it is understood that the insertion force with peg rotation become very small comparing to that without peg rotation. The periodicity observed on the experimental insertion force is due to the misalignment between the peg axis and rotary axis.

From this experiments, it is shown that the peg rotation is very effective to decrease the insertion force.

7. CONCLUSIONS

Two methods to make smooth insertion between round peg and hole are proposed. One of them is the method to use minimum insertion force by using RCC with optimum position of the compliance center with known insertion angle. The other is to decrease the friction coefficient by peg rotation of the usual RCC. The dynamical characteristics of two methods were analyzed theoretically and their design methods were derived. They are proved to be valid for decreasing the insertion force experimentally.

ACKNOWLEDGMENT

This work was financially supported in part by a Grant-in-Aid for Scientific Research,the Ministry of Education, Scientific and Culture of Japan, No.62850043.

Reference

[1] D.E.Whitney & J.L.Nevins "WHAT IS THE RCC AND WHAT CAN IT DO?", Proc. of 9th ISIR, pp 135-152

[2]D.E.Whitney,"Part Mating in Assembly" , Handbook of Industrial Robotics, John Wiley & Sons. Inc,1985, pp. 1084-1114

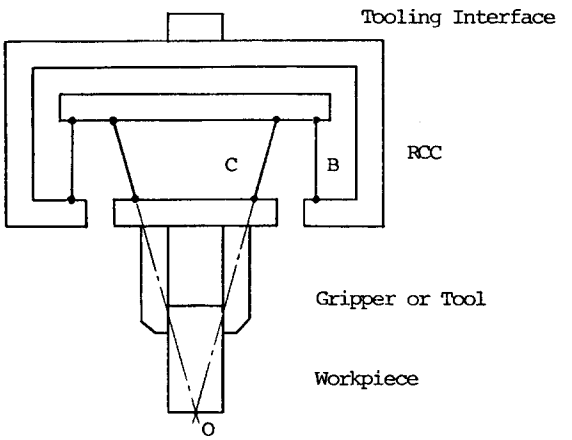

Fig.1 2 dimensional model of RCC

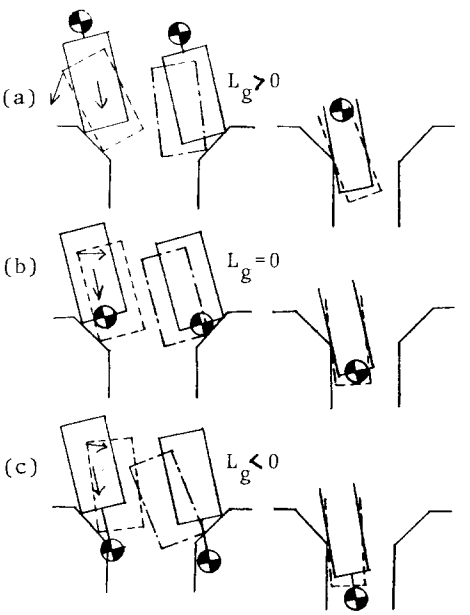

Fig.2 Insertion mechanism of peg and hole using RCC

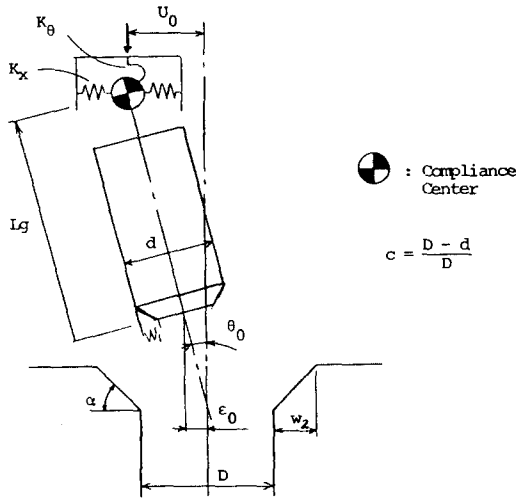

Fig.3 Definitions of terms for part mating

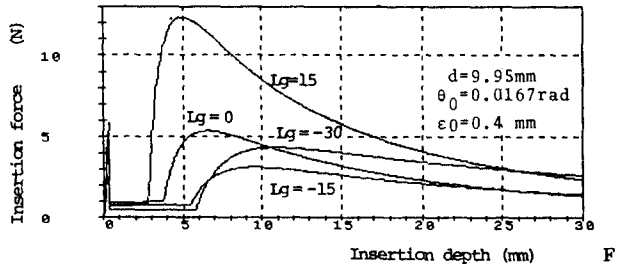

Fig.5 Comparisons between insertion force for various Lg

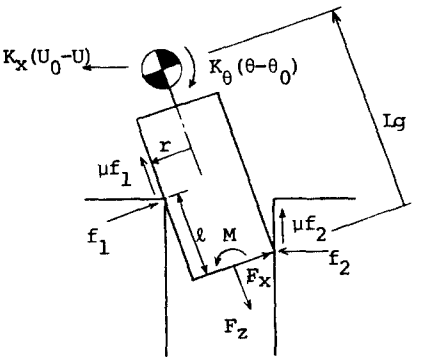

Fig.4 Forces acting during two points contact

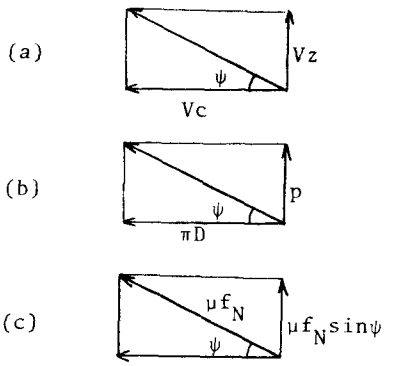

Fig.7 Several relations at the insertion with peg rotation

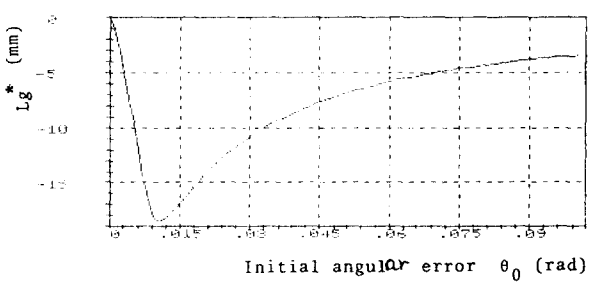

Fig.6 Optimum Lg* versus θ_o

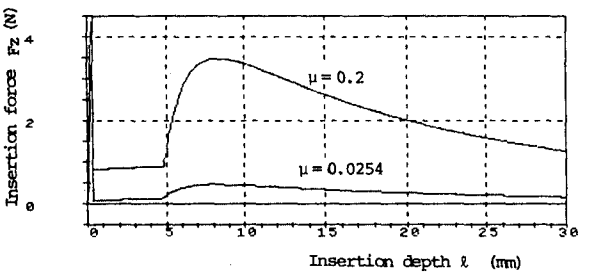

Fig.8 Comparison between insertion forces at the peg insertions with and without peg rotation

Table1

Kx	12 N/mm
Kθ	12000 N-mm/rad
μ	0.2
w	0.5 mm
α	45°

Table2

軸の直径 d(mm)	9.9	9.95	9.99
軸の長さ a(mm)	55	85	30

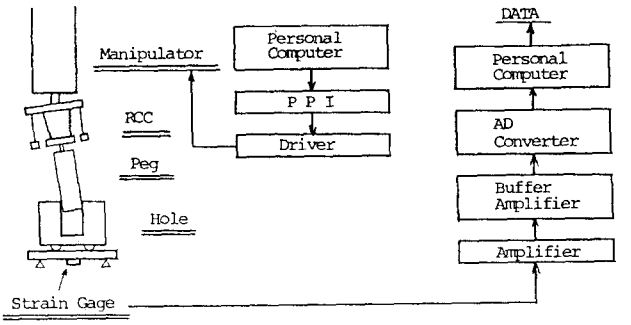

Fig.9 Schematic diagram of experimental system

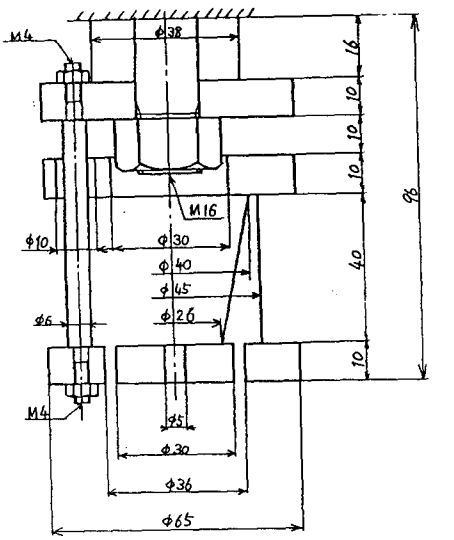

Fig.10 RCC used in the experiment

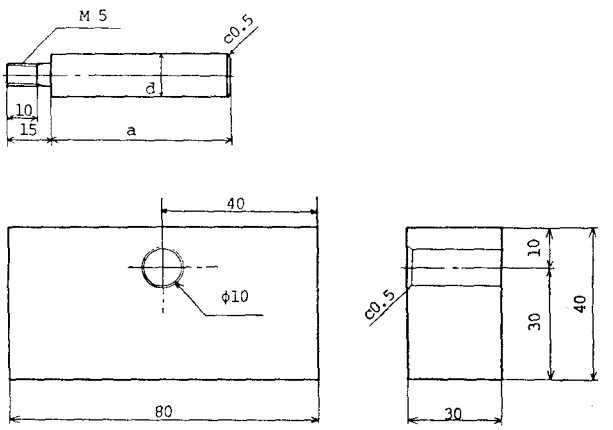

Fig.11 Dimensions of peg and hole

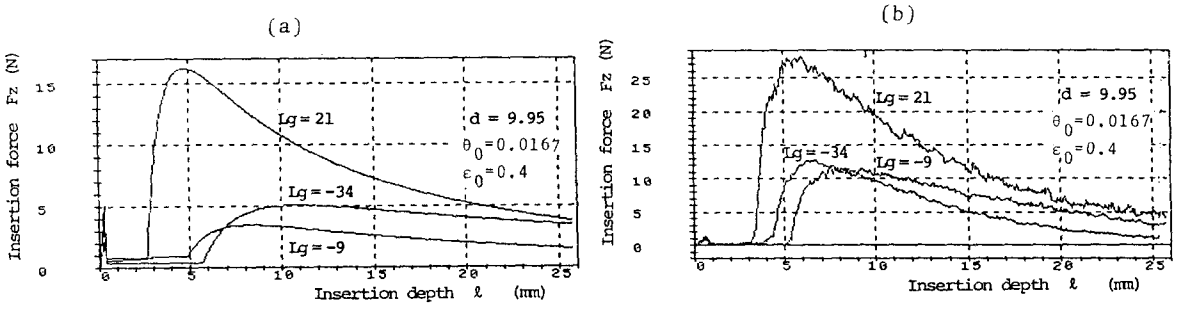

Fig.12 Theoretical and experimental insertion forces

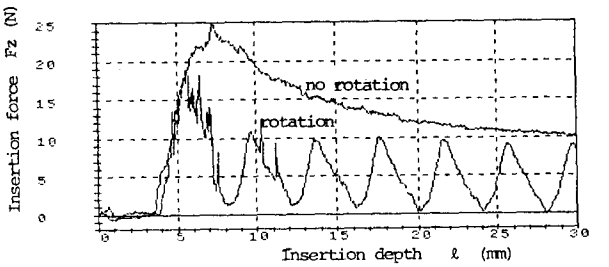

Fig.13 Comparison between the experimental insertion forces with and without rotation of peg